THE JOURNAL OF PHYSICAL CHEMISTRY Letters

Letter

pubs.acs.org/JPCL

Solid-State Mesostructured Perovskite $CH_3NH_3PbI_3$ Solar Cells: Charge Transport, Recombination, and Diffusion Length

Yixin Zhao, Alexandre M. Nardes, and Kai Zhu*

Chemical and Materials Science Center, National Renewable Energy Laboratory, 15013 Denver West Parkway, Golden, Colorado 80401, United States

Supporting Information

ABSTRACT: We report on the effect of TiO_2 film thickness on charge transport and recombination in solid-state mesostructured perovskite $CH_3NH_3PbI_3$ (via one-step coating) solar cells using spiro-MeOTAD as the hole conductor. Intensity-modulated photocurrent/photovoltage spectroscopies show that the transport and recombination properties of solid-state mesostructured perovskite solar cells are similar to those of solid-state dye-sensitized solar cells. Charge transport in perovskite cells is dominated by electron conduction within the mesoporous TiO_2 network rather than from the perovskite layer. Although no significant film-thickness dependence is found for transport and recombination, the efficiency of perovskite cells increases with TiO_2 film thickness from 240 nm to about 650−850 nm owing primarily to the enhanced light harvesting. Further increasing film thickness reduces cell efficiency associated with decreased fill factor or photocurrent density. The electron diffusion length in mesostructured perovskite cells is longer than 1 μm for over four orders of magnitude of light intensity.

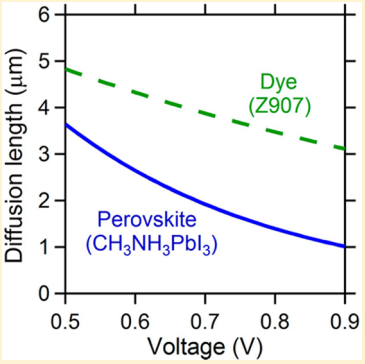

SECTION: Energy Conversion and Storage; Energy and Charge Transport

Organometallic halide perovskites (e.g., $CH_3NH_3PbI_3$ and $CH_3NH_3PbI_{3-x}Cl_x$) have recently emerged as a new class of light absorbers that have demonstrated exceptional progress in solar cell performance.[1,2] Efficiencies over 15% have been reported[3,4] since their first use in solar cells in 2009.[5] Such high-efficiency perovskite cells can be made by either solution processing or thermal evaporation. These promising results have made halide perovskites one of the most attractive light-absorbing materials for solar conversion applications.[6−16] Two types of device architectures (i.e., mesostructured or bilayer thin-film solar cells) are normally used for halide perovskites. The first type is adapted from solid-state dye-sensitized solar cells (DSSCs), in which a mesoporous metal oxide (e.g., TiO_2) provides a large surface area to support the perovskite absorber and spiro-MeOTAD is normally used as the hole transport material (HTM).[3,8,9,15,17,18] The device also works well in the absence of the HTM layer.[19] In the second type, the bulk thin-film perovskite absorber layer is sandwiched between the electron- and hole-contact layers (e.g., TiO_2 and spiro-MeOTAD, respectively).[4,20] Despite the rapid progress in device performance, understanding the structural and electronic properties of halide perovskites is just in its infancy. One of the key determinants of solar cell performance is the charge-carrier diffusion length (L_d). A longer L_d generally means a thicker absorber layer for greater light harvesting. Recent studies have shown that for the planar perovskite cell structure, both electron and hole diffusion lengths are >1 μm for $CH_3NH_3PbI_{3-x}Cl_x$[21] and >100 nm for $CH_3NH_3PbI_3$.[22] However, the charge-carrier diffusion length has not been determined for the solid-state mesostructured perovskite cells, even though such a cell structure has led to the highest certified perovskite solar cell efficiencies so far. Because the solid-state mesostructured perovskite solar cell resembles the solid-state DSSC,[23,24] several studies report on the transport properties of mesostructured perovskite cells using common characterization techniques from the DSSC field, such as transient photocurrent/photovoltage decay[9,15] and impedance spectroscopy (IS).[16,25,26] One study shows that the transport time in mesostructured perovskite cells depends little on the hole mobility of HTM (varying over five orders of magnitude),[15] suggesting that transport in these cells is limited by electron conduction. Another study suggests that electron transport could take place in the mesoporous metal oxide layer (e.g., TiO_2) or in the perovskite layer itself.[9]

Herein we present results of our investigation on the effect of TiO_2 film thickness on charge transport, recombination, and device characteristics of solid-state mesostructured perovskite $CH_3NH_3PbI_3$ solar cells using spiro-MeOTAD as the hole conductor. Charge transport and recombination are examined by intensity-modulated photocurrent/photovoltage spectroscopies (IMPS/IMVS). We find that the transport and recombination properties of solid-state mesostructured perovskite $CH_3NH_3PbI_3$ solar cells are similar to those of solid-state Z907-based DSSC. The electron diffusion length in mesostructured perovskite cells is longer than 1 μm under normal cell operation conditions.

Received: January 1, 2014
Accepted: January 20, 2014
Published: January 20, 2014

Figure 1 shows typical cross-sectional scanning electron microscopy (SEM) images of solid-state mesostructured TiO_2/$CH_3NH_3PbI_3$/spiro-MeOTAD solar cells. The average TiO_2 film thickness (as determined from a surface profiler) ranges from 240 to 1650 nm. For each sample in this study a spiro-MeOTAD overlayer is seen on the top surface of the mesoporous TiO_2 layer. The thickness of this HTM capping layer decreases from about 500 to 350 nm when the TiO_2 film thickness increases from 240 to 1650 nm. The thickness range of the HTM capping layer is consistent with literature reports.[4,8,9,25] The typical X-ray diffraction (XRD) patterns and ultraviolet−visible (UV−vis) absorption spectra (Figure S1 in the Supporting Information) for the perovskite $CH_3NH_3PbI_3$ agree with our previous studies.[27,28] The absorption spectrum of the $CH_3NH_3PbI_3$-sensitized mesoporous TiO_2 film increases for thicker TiO_2 films, corresponding to an enhanced loading of $CH_3NH_3PbI_3$.

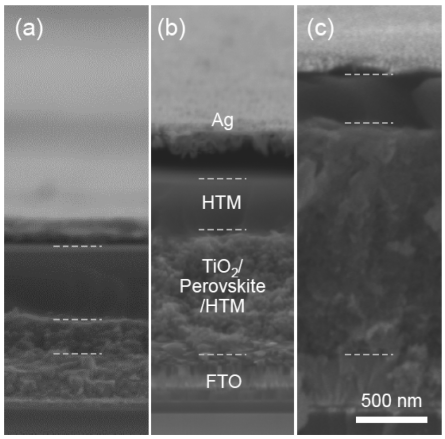

Figure 1. Typical cross-sectional SEM images of solid-state mesostructured TiO_2/$CH_3NH_3PbI_3$/spiro-MeOTAD solar cells with different TiO_2 film thicknesses. Three representative TiO_2 film thicknesses are shown in panels a−c, respectively.

Table 1 compares the $J-V$ characteristics of solid-state mesostructured perovskite $CH_3NH_3PbI_3$ solar cells with different TiO_2 film thicknesses measured under simulated AM 1.5G 100 mW/cm^2. The $J-V$ and IPCE curves as a function of TiO_2 film thickness are, respectively, shown in Figures S2 and S3 (Supporting Information). The cell efficiency first increases from about 5 to 9% when the TiO_2 film thickness is changed from 240 nm to the range of 650−850 nm. Further increasing film thickness results in lower cell efficiencies. The initial increase in the cell efficiency with increasing film thickness is consistent with the enhanced light absorption (Figure S1 in the Supporting Information). The decrease in cell efficiency for TiO_2 films thicker than 1 μm is primarily caused by the reduced FF or J_{sc}, despite the enhanced absorption for thicker TiO_2 films. The significant drop of FF for TiO_2 films thicker than 1 μm is likely caused by the reduced pore filling of spiro-MeOTAD within the mesoporous TiO_2 films. It is worth noting that the maximum efficiency for a perovskite $CH_3NH_3PbI_3$ solar cell using a 650 nm TiO_2 film in this study is 10.3% with a J_{sc} of 17.8 mA/cm^2, V_{oc} of 0.90 V, and FF of 0.64 ($J-V$ and IPCE curves shown in Figure S4 in the Supporting Information). In contrast, a solid-state DSSC using the Z907 dye and 650 nm TiO_2 film shows a J_{sc} of 4.5 mA/cm^2, V_{oc} of 0.77 V, and FF of 0.63 to yield an efficiency of 2.2%. The efficiency difference between the perovskite cell and DSSC results primarily from their markedly different J_{sc} values associated with their respective light-absorption properties.[6]

Table 1. Effect of TiO_2 Film Thickness on Short-Circuit Photocurrent Density (J_{sc}), Open-Circuit Voltage (V_{oc}), Fill Factor (FF), and Conversion Efficiency η of Solid-State Perovskite $CH_3NH_3PbI_3$ Solar Cells

thickness (nm)	J_{sc} (mA/cm^2)	V_{oc} (V)	FF	η (%)
240	10.41	0.851	0.577	5.11
300	11.13	0.859	0.593	5.67
400	13.11	0.871	0.548	6.26
500	15.36	0.869	0.536	7.16
650	17.57	0.889	0.567	8.85
850	17.69	0.890	0.555	8.73
1050	17.16	0.878	0.490	7.39
1650	14.17	0.869	0.445	5.48

Figure 2a shows the effect of TiO_2 film thickness on the electron diffusion coefficient (D) for the solid-state mesostructured perovskite $CH_3NH_3PbI_3$ solar cells as a function of photoelectron density (n). The D values are calculated from transport times (τ_t) determined by IMPS measurements at short circuit.[29] The diffusion coefficients for a Z907-sensitized solid-state dye cell based on the 650-nm TiO_2 film are also plotted for comparison. The D values can be fitted to a power-law dependence on n following an expression $D \propto n^{1/\alpha-1}$ with α = 0.49 for all samples. Such power-law dependence in DSSCs has been attributed to multiple trapping and detrapping of electrons during their transit through the TiO_2 network.[30−35] There is no obvious thickness dependence of the D values among perovskite solar cells. The diffusion coefficients for the perovskite cell with a 650 nm TiO_2 film are essentially the same as that for the solid-state DSSC with the same TiO_2 film thickness. These results indicate that the mechanistic factors governing the charge transport in the solid-state $CH_3NH_3PbI_3$ solar cells are similar to those in the solid-state DSSCs, suggesting that transport in the perovskite cells is dominated by the electron conduction within the TiO_2 network rather than from the perovskite layer itself. Figure 2b shows the recombination lifetime (τ_r) as a function of quasi-Fermi level (or open-circuit voltage). The τ_r values are determined by IMVS measurements at open circuit.[29] All perovskite cells and the DSSC exhibit essentially the same voltage dependence of recombination lifetime. The τ_r value decreases with increasing voltage for all samples; for DSSCs, such dependence is normally attributed to the enhanced recombination with the higher electron density.[29] For a given voltage, there is no noticeable difference of τ_r among perovskite cells with different TiO_2 film thickness, suggesting that recombination occurs homogenously across the mesoporous TiO_2 film.[36,37] Moreover, no difference in τ_r is observed between the perovskite cells and DSSC, implying that recombination kinetics does not depend on the absorber deposited on the TiO_2 surface in this study. This observation significantly differs from a recent study on solid-state perovskite cells using ZnO nanorods, where recombination is found to increase with the length of ZnO nanorods.[38]

From the measurements of transport and recombination times (τ_t and τ_r, respectively), one can determine the electron diffusion length L_d in the solid-state mesostructured perovskite $CH_3NH_3PbI_3$ solar cells by using the expression $L_d = d(\tau_r/\tau_t)^{1/2}$ (where d is the TiO_2 film thickness). The electron diffusion

dx.doi.org/10.1021/jz500003v | J. Phys. Chem. Lett. 2014, 5, 490−494

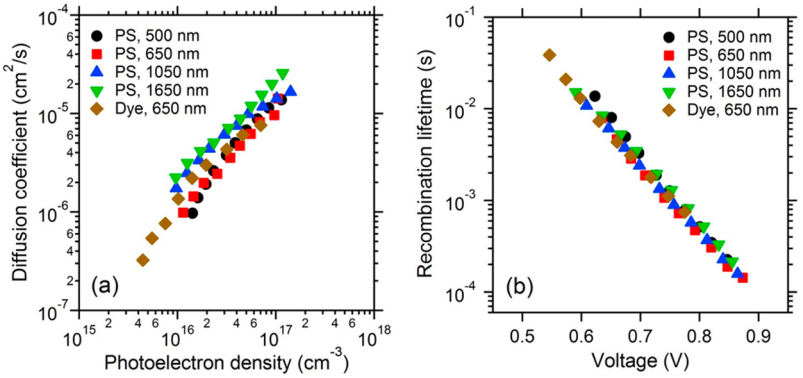

Figure 2. (a) Electron diffusion coefficient as a function of photoelectron density. (b) Recombination lifetime as a function of open-circuit voltage. PS: perovskite $CH_3NH_3PbI_3$; Dye: Z907 dye.

length in DSSC is a measure of the average distance an electron travels before it recombines with either the oxidized absorber or the hole conductor.[39] A longer L_d could lead to higher charge-collection or light-harvesting efficiencies for an improved solar conversion efficiency. Figure 3a shows the dependence of

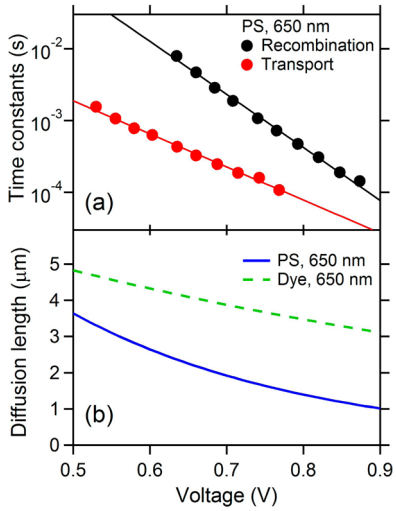

Figure 3. (a) Comparison of transport and recombination times for a mesostructured perovskite solar cell as a function of voltage (or quasi-Fermi level). (b) Comparison of the electron diffusion length for a mesostructured perovskite cell and a solid-state DSSC using 650 nm TiO_2 films. PS: perovskite $CH_3NH_3PbI_3$; Dye: Z907 dye.

transport and recombination times on voltage (or quasi-Fermi level QFL) for a solid-state mesostructured perovskite solar cell using a 650 nm thick TiO_2 film. The QFL at open circuit is given by the open-circuit voltage, whereas the average QFL at short circuit for a given light intensity is determined by a switching method reported previously for DSSCs.[40] Figure 3b shows the L_d values as a function of QFL for the perovskite solar cell. The diffusion length decreases from about 3.5 to 1 μm when the QFL increases from 0.5 to 0.9 V (corresponding to over four orders of magnitude of light intensity). In comparison, L_d for a solid-state Z907-based DSSC exhibits a similar dependence on QFL, which is in agreement with a previous report on solid-state DSSCs.[41] Although L_d for the solid-state DSSC is longer than that for the perovskite cell over the entire voltage range, the lower absorption property of dye molecules compared with perovskites limits the performance of solid-state DSSCs. The observed voltage dependence of L_d implies that charge collection should, in general, be more efficient at lower light intensity for mesostructured perovskite cells. Because the average QFLs at short circuit (under simulated AM 1.5G 100 mW/cm^2) for perovskite cells are around 0.75 to 0.8 V in this study, the L_d values are thus expected to be about 1.2 to 1.5 μm (Figure 3b), implying that charge collection at short circuit should not limit solar conversion efficiency for all perovskite samples except for the one using a 1.65 μm TiO_2 film. This is consistent with the J_{sc} dependence on the TiO_2 film thickness (Figure S2 in the Supporting Information). A poorer pore filling of spiro-MeOTAD for thicker TiO_2 films could also contribute to the observed low performance (e.g., FF or J_{sc}) for the perovskite cell based on thicker TiO_2 films (Table 1).[41]

In summary, we examined charge transport, recombination, and device characteristics of solid-state mesostructured perovskite $CH_3NH_3PbI_3$ solar cells based on 0.24 to 1.65 μm thick TiO_2 films and spiro-MeOTAD hole conductor. Charge transport and recombination in the solid-state mesostructured perovskite cells are similar to those in the solid-state DSSC and exhibit little dependence on the TiO_2 film thickness. The performance of perovskite cells increases with TiO_2 film thickness up to 650−850 nm, resulting primarily from the enhanced light harvesting. Further increasing film thickness results in lower cell efficiencies, mainly caused by the reduced FF or J_{sc}. The electron diffusion length in mesostructured perovskite cells is found to be longer than 1 μm under normal cell operation conditions.

■ ASSOCIATED CONTENT

Supporting Information

Experimental method, XRD and UV−vis spectra, J−V and IPCE curves as a function of TiO_2 film thickness, optimized J−V characteristics, and IPCE spectrum. This material is available free of charge via the Internet at http://pubs.acs.org.

■ AUTHOR INFORMATION

Corresponding Author

*E-mail: Kai.Zhu@nrel.gov.

Notes

The authors declare no competing financial interest.

■ ACKNOWLEDGMENTS

This work was supported by the Division of Chemical Sciences, Geosciences, and Biosciences, Office of Basic Energy Sciences,

U.S. Department of Energy, under contract No. DE-AC36-08-GO28308 with the National Renewable Energy Laboratory.

REFERENCES

(1) Park, N. G. Organometal Perovskite Light Absorbers Toward a 20% Efficiency Low-Cost Solid-State Mesoscopic Solar Cell. *J. Phys. Chem. Lett.* **2013**, *4*, 2423−2429.

(2) Snaith, H. J. Perovskites: The Emergence of a New Era for Low-Cost, High-Efficiency Solar Cells. *J. Phys. Chem. Lett.* **2013**, 3623−3630.

(3) Burschka, J.; Pellet, N.; Moon, S. J.; Humphry-Baker, R.; Gao, P.; Nazeeruddin, M. K.; Gratzel, M. Sequential Deposition as a Route to High-Performance Perovskite-Sensitized Solar Cells. *Nature* **2013**, *499*, 316−319.

(4) Liu, M.; Johnston, M. B.; Snaith, H. J. Efficient Planar Heterojunction Perovskite Solar Cells by Vapour Deposition. *Nature* **2013**, *501*, 395−398.

(5) Kojima, A.; Teshima, K.; Shirai, Y.; Miyasaka, T. Organometal Halide Perovskites as Visible-Light Sensitizers for Photovoltaic Cells. *J. Am. Chem. Soc.* **2009**, *131*, 6050−6051.

(6) Im, J.-H.; Lee, C.-R.; Lee, J.-W.; Park, S.-W.; Park, N.-G. 6.5% Efficient Perovskite Quantum-Dot-Sensitized Solar Cell. *Nanoscale* **2011**, *3*, 4088−4093.

(7) Etgar, L.; Gao, P.; Xue, Z.; Peng, Q.; Chandiran, A. K.; Liu, B.; Nazeeruddin, M. K.; Grätzel, M. Mesoscopic $CH_3NH_3PbI_3/TiO_2$ Heterojunction Solar Cells. *J. Am. Chem. Soc.* **2012**, *134*, 17396−17399.

(8) Kim, H.-S.; Lee, C.-R.; Im, J.-H.; Lee, K.-B.; Moehl, T.; Marchioro, A.; Moon, S.-J.; Humphry-Baker, R.; Yum, J.-H.; Moser, J. E.; et al. Lead Iodide Perovskite Sensitized All-Solid-State Submicron Thin Film Mesoscopic Solar Cell with Efficiency Exceeding 9%. *Sci. Rep.* **2012**, *2*, 591.

(9) Lee, M. M.; Teuscher, J.; Miyasaka, T.; Murakami, T. N.; Snaith, H. J. Efficient Hybrid Solar Cells Based on Meso-Superstructured Organometal Halide Perovskites. *Science* **2012**, *338*, 643−647.

(10) Edri, E.; Kirmayer, S.; Cahen, D.; Hodes, G. High Open-Circuit Voltage Solar Cells Based on Organic−Inorganic Lead Bromide Perovskite. *J. Phys. Chem. Lett.* **2013**, *4*, 897−902.

(11) Cai, B.; Xing, Y.; Yang, Z.; Zhang, W.-H.; Qiu, J. High Performance Hybrid Solar Cells Sensitized by Organolead Halide Perovskites. *Energy Environ. Sci.* **2013**, *6*, 1480−1485.

(12) Qiu, J.; Qiu, Y.; Yan, K.; Zhong, M.; Mu, C.; Yan, H.; Yang, S. All-Solid-State Hybrid Solar Cells Based on a New Organometal Halide Perovskite Sensitizer and One-Dimensional TiO_2 Nanowire Arrays. *Nanoscale* **2013**, *5*, 3245−3248.

(13) Noh, J. H.; Im, S. H.; Heo, J. H.; Mandal, T. N.; Seok, S. I. Chemical Management for Colorful, Efficient, and Stable Inorganic−Organic Hybrid Nanostructured Solar Cells. *Nano Lett.* **2013**, *13*, 1764−1769.

(14) Docampo, P.; Ball, J. M.; Darwich, M.; Eperon, G. E.; Snaith, H. J. Efficient Organometal Trihalide Perovskite Planar-Heterojunction Solar Cells on Flexible Polymer Substrates. *Nat. Commun.* **2013**, *4*, 2761.

(15) Bi, D.; Yang, L.; Boschloo, G.; Hagfeldt, A.; Johansson, E. M. J. Effect of Different Hole Transport Materials on Recombination in $CH_3NH_3PbI_3$ Perovskite-Sensitized Mesoscopic Solar Cells. *J. Phys. Chem. Lett.* **2013**, *4*, 1532−1536.

(16) Christians, J. A.; Fung, R. C. M.; Kamat, P. V. An Inorganic Hole Conductor for Organo-Lead Halide Perovskite Solar Cells. Improved Hole Conductivity with Copper Iodide. *J. Am. Chem. Soc.* **2014**, *136*, 758−764.

(17) Kim, H. S.; Lee, J. W.; Yantara, N.; Boix, P. P.; Kulkarni, S. A.; Mhaisalkar, S.; Gratzel, M.; Park, N. G. High Efficiency Solid-State Sensitized Solar Cell-Based on Submicrometer Rutile TiO_2 Nanorod and $CH_3NH_3PbI_3$ Perovskite Sensitizer. *Nano Lett.* **2013**, *13*, 2412−2417.

(18) Heo, J. H.; Im, S. H.; Noh, J. H.; Mandal, T. N.; Lim, C. S.; Chang, J. A.; Lee, Y. H.; Kim, H. J.; Sarkar, A.; Nazeeruddin, M. K.; et al. Efficient Inorganic-Organic Hybrid Heterojunction Solar Cells Containing Perovskite Compound and Polymeric Hole Conductors. *Nat. Photonics* **2013**, *7*, 487−492.

(19) Abu Laban, W.; Etgar, L. Depleted Hole Conductor-Free Lead Halide Iodide Heterojunction Solar Cells. *Energy Environ. Sci.* **2013**, *6*, 3249−3253.

(20) Jeng, J. Y.; Chiang, Y. F.; Lee, M. H.; Peng, S. R.; Guo, T. F.; Chen, P.; Wen, T. C. $CH_3NH_3PbI_3$ Perovskite/Fullerene Planar-Heterojunction Hybrid Solar Cells. *Adv. Mater.* **2013**, *25*, 3727−3732.

(21) Stranks, S. D.; Eperon, G. E.; Grancini, G.; Menelaou, C.; Alcocer, M. J. P.; Leijtens, T.; Herz, L. M.; Petrozza, A.; Snaith, H. J. Electron-Hole Diffusion Lengths Exceeding 1 Micrometer in an Organometal Trihalide Perovskite Absorber. *Science* **2013**, *342*, 341−344.

(22) Xing, G.; Mathews, N.; Sun, S.; Lim, S. S.; Lam, Y. M.; Gratzel, M.; Mhaisalkar, S.; Sum, T. C. Long-Range Balanced Electron- and Hole-Transport Lengths in Organic-Inorganic $CH_3NH_3PbI_3$. *Science* **2013**, *342*, 344−347.

(23) Cai, N.; Moon, S.-J.; Cevey-Ha, L.; Moehl, T.; Humphry-Baker, R.; Wang, P.; Zakeeruddin, S. M.; Graltzel, M. An Organic D-π-A Dye for Record Efficiency Solid-State Sensitized Heterojunction Solar Cells. *Nano Lett.* **2011**, *11*, 1452−1456.

(24) Jang, S. R.; Zhu, K.; Ko, M. J.; Kim, K.; Kim, C.; Park, N. G.; Frank, A. J. Voltage-Enhancement Mechanisms of an Organic Dye in High Open-Circuit Voltage Solid-State Dye-Sensitized Solar Cells. *ACS Nano* **2011**, *5*, 8267−8274.

(25) Kim, H. S.; Mora-Sero, I.; Gonzalez-Pedro, V.; Fabregat-Santiago, F.; Juarez-Perez, E. J.; Park, N. G.; Bisquert, J. Mechanism of Carrier Accumulation in Perovskite Thin-Absorber Solar Cells. *Nat. Commun.* **2013**, *4*, 2242.

(26) Dualeh, A.; Moehl, T.; Tétreault, N.; Teuscher, J.; Gao, P.; Nazeeruddin, M. K.; Grätzel, M. Impedance Spectroscopic Analysis of Lead Iodide Perovskite-Sensitized Solid-State Solar Cells. *ACS Nano* **2014**, DOI: 10.1021/nn404323g.

(27) Zhao, Y.; Zhu, K. Charge Transport and Recombination in Perovskite $(CH_3NH_3)PbI_3$ Sensitized TiO_2 Solar Cells. *J. Phys. Chem. Lett.* **2013**, *4*, 2880−2884.

(28) Zhao, Y.; Zhu, K. Optical Bleaching of Perovskite (CH_3NH_3)-PbI_3 Through Room-Temperature Phase Transformation Induced by Ammonia. *Chem. Commun.* **2014**, *50*, 1605−1607.

(29) Zhu, K.; Jang, S.-R.; Frank, A. J. Impact of High Charge-Collection Efficiencies and Dark Energy-Loss Processes on Transport, Recombination, and Photovoltaic Properties of Dye-Sensitized Solar Cells. *J. Phys. Chem. Lett.* **2011**, *2*, 1070−1076.

(30) Nelson, J.; Haque, S. A.; Klug, D. R.; Durrant, J. R. Trap-Limited Recombination in Dye-Sensitized Nanocrystalline Metal Oxide Electrodes. *Phys. Rev. B* **2001**, *63*, 205321.

(31) Dloczik, L.; Ileperuma, O.; Lauermann, I.; Peter, L. M.; Ponomarev, E. A.; Redmond, G.; Shaw, N. J.; Uhlendorf, I. Dynamic Response of Dye-Sensitized Nanocrystalline Solar Cells: Characterization by Intensity-Modulated Photocurrent Spectroscopy. *J. Phys. Chem. B* **1997**, *101*, 10281−10289.

(32) Solbrand, A.; Lindstrom, H.; Rensmo, H.; Hagfeldt, A.; Lindquist, S. E.; Sodergren, S. Electron Transport in the Nanostructured TiO_2-Electrolyte System Studied with Time-Resolved Photocurrents. *J. Phys. Chem. B* **1997**, *101*, 2514−2518.

(33) Bisquert, J.; Vikhrenko, V. S. Interpretation of the Time Constants Measured by Kinetic Techniques in Nanostructured Semiconductor Electrodes and Dye-Sensitized Solar Cells. *J. Phys. Chem. B* **2004**, *108*, 2313−2322.

(34) Barzykin, A. V.; Tachiya, M. Mechanism of Charge Recombination in Dye-Sensitized Nanocrystalline Semiconductors: Random Flight Model. *J. Phys. Chem. B* **2002**, *106*, 4356−4363.

(35) Zhu, K.; Kopidakis, N.; Neale, N. R.; van de Lagemaat, J.; Frank, A. J. Influence of Surface Area on Charge Transport and Recombination in Dye-Sensitized TiO_2 Solar Cells. *J. Phys. Chem. B* **2006**, *110*, 25174−25180.

(36) Zhu, K.; Schiff, E. A.; Park, N.-G.; Lagemaat, J. v. d.; Frank, A. J. Determining the Locus for Photocarrier Recombination in Dye-Sensitized Solar Cells. *Appl. Phys. Lett.* **2002**, *80*, 685−687.

(37) Zhu, K.; Neale, N. R.; Miedaner, A.; Frank, A. J. Enhanced Charge-Collection Efficiencies and Light Scattering in Dye-Sensitized Solar Cells Using Oriented TiO_2 Nanotubes Arrays. *Nano Lett.* **2006**, *7*, 69−74.
(38) Bi, D. Q.; Boschloo, G.; Schwarzmuller, S.; Yang, L.; Johansson, E. M. J.; Hagfeldt, A. Efficient and Stable $CH_3NH_3PbI_3$-Sensitized ZnO Nanorod Array Solid-State Solar Cells. *Nanoscale* **2013**, *5*, 11686−11691.
(39) Frank, A. J.; Kopidakis, N.; van de Lagemaat, J. Electrons in Nanostructured TiO_2 Solar Cells: Transport, Recombination and Photovoltaic Properties. *Coord. Chem. Rev.* **2004**, *248*, 1165−1179.
(40) Boschloo, G.; Hagfeldt, A. Activation Energy of Electron Transport in Dye-Sensitized TiO_2 Solar Cells. *J. Phys. Chem. B* **2005**, *109*, 12093−12098.
(41) Jennings, J. R.; Peter, L. M. A Reappraisal of the Electron Diffusion Length in Solid-State Dye-Sensitized Solar Cells. *J. Phys. Chem. C* **2007**, *111*, 16100−16104.